Flame Propagation in Poiseuille Flow under Adiabatic Conditions

J. DAOU[†] and M. MATALON*

Department of Engineering Sciences and Applied Mathematics, Northwestern University, Evanston, IL 60208-3125, USA

We describe flame propagation in a channel subject to a Poiseuille flow, within the thermo-diffusive approximation and an adiabatic context. The two-dimensional flame fronts addressed may be either assisted or opposed by the flow. The problem is characterized by two parameters, the intensity of the flow u_0 and the spatial scale ϵ. The total burning rate and the propagation speed are determined in terms of u_0 and ϵ and different distinguished regimes are described. From the results, simple criteria for flame flashback in channels are identified. Conclusions concerning the long-term evolution of an ignition kernel in the present flow are also drawn. The results may also be useful in interpreting similar features encountered in more complicated flow situations. For example, the quadratic dependence of the burning rate on u_0 for weak flow intensities, and linear dependence for larger u_0, is similar to that of the turbulent flame speed when the latter is considered as a function of the velocity fluctuations or turbulence intensity.

INTRODUCTION

In this work, we describe the two-dimensional traveling waves associated with flame propagation in a combustible mixture subject to a Poiseuille flow. Despite the fundamental importance of this flow and its high relevance in combustion applications (such as Bunsen burners), it does not seem to have received due attention with regards to the evolution of freely propagating deflagrations in it. In contrast, previous consideration has been devoted to the stationary flame case in this context, mainly in connection with the problem of flame anchoring at the exit of a Bunsen burner (cf. [1–3]). Stationary flames exist only for a restricted range of flow intensity between a flashback and a blowoff values. Outside this range, flame propagation opposed to or assisted by the flow may occur.

For stationary flames stabilized at the exit of a Bunsen burner, heat losses to the burner's rim play a crucial role in "holding" the flame. By decreasing the losses the flame may move into the tube, a phenomenon known as "flashback". This could be achieved, for example, by heating the walls of the burner, which may be induced by the flame itself. Flashback conditions are not desirable for design purpose and are serious safety hazard. Therefore, it is important to determine the conditions under which flashback is suppressed. This will be identified in this work as the conditions under which flame propagation opposing the flow is no longer possible. Although such conditions depend, in general, on the heat transfer rate to the walls, we shall neglect such effects in the present paper and consider them in later publications. For the adiabatic conditions considered here, we therefore shall identify what may be considered as *sufficient conditions* for the nonoccurrence of flame flashback, which are expected to be valid even in the presence of heat losses. We note parenthetically that we are concerned here with the *steady* propagation case and do not address questions concerning flame stability.

Another issue that we address in this study is the evolution of a localized ignition spot in Poiseuille flow, which could be viewed as a particular case of the practically important and poorly understood problem of ignition in a prescribed flow field. Consider, for instance, a hot kernel of burned gas generated at initial time, say by a strong spark, in an infinitely long channel (see Fig. 1). Even when ignition is successful, the conditions for flame propagation depend, on the intensity and the scale of the flow field. Our goal is to determine the longtime evolution described by the two flame fronts shown in Fig. 1b; the front to the right, which is

*Corresponding author. E-mail: matalon@nwu.edu
[†]Current address: UMIST, Department of Mathematics, Manchester M60 1QD, UK; Email: j.daou@umist.ac.uk

COMBUSTION AND FLAME 124:337–349 (2001)

Published by Elsevier Science Inc.
0010-2180/01/$–see front matter
PII S0010-2180(00)00209-1

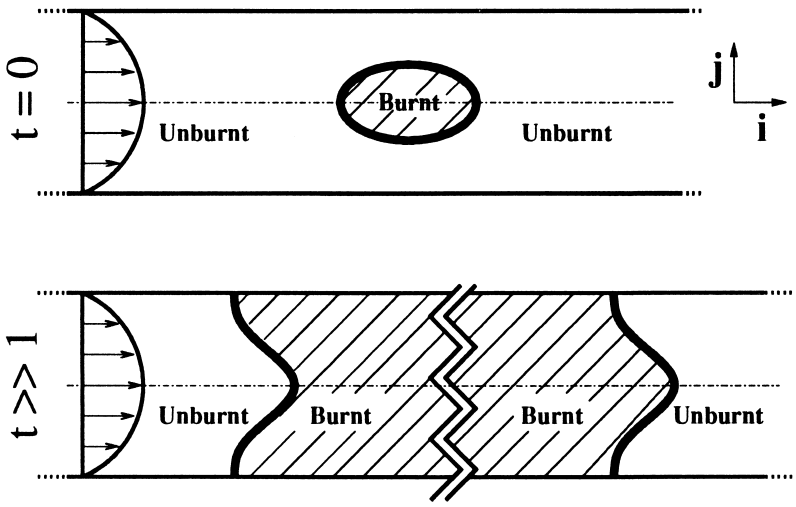

Fig. 1. Skematic of flame development from an initial hot kernel of burnt gas in a Poiseuille flow. The top subfigure depicts the situation at initial time, $t = 0$. The bottom subfigure corresponds to $t \gg 1$ and shows two flame fronts, the left one propagating against the flow and the right one in the flow direction.

assisted, and the one to the left, which is opposed by the flow. The only study that addresses a similar problem is that of Dery [4], who used a simple kinematic approach to examine the evolution preceding the flame establishment at the exit of a Bunsen burner.

In studying freely propagating deflagrations in Poiseuille flow, we shall concentrate on the influence of two parameters, namely the channel width relative to the flame thickness and the maximum flow velocity relative to the laminar flame speed. These can advantageously be thought of as representing in general the typical spatial scale and magnitude of the velocity fluctuation (from its mean value). Because of the simplicity of Poiseuille flow, their combined effects may be studied with some detail, both theoretically and experimentally. This may provide insight into more complex situations characterized by similar parameters, such as the interaction between an eddy of a given characteristic size and speed with the flame. Such point of view has been made previously by others (see for example [5]–[7]) who have used spatially sinusoidal flows with prescribed wavelength and amplitude to explain certain aspects of turbulent combustion. This approach may substantially complement that based on the counterflow configuration, which is characterized by a single parameter, the strain rate, rather than independent length and velocity scales.

The paper is structured as follows. We begin by formulating the problem in the context of the thermo-diffusive model of constant density and constant transport properties. Unity Lewis number is assumed and adiabatic conditions are considered. A simple model is first written for the situation corresponding to a weakly stretched flame, but which retains two independent parameters for the characterization of the scale and intensity of the flow. Analytical results for different distinguished limits are thus derived. Next, numerical results of the full two-dimensional problem are presented along with conclusions that address the issues introduced above.

FORMULATION

We consider flame propagation in an infinitely long channel of width $2R$, under a prescribed Poiseuille flow as shown in Fig. 2. Within the constant-density approximation adopted, the flow is unaffected by the combustion process. The fluid velocity is given by $\tilde{u}_0(1 - Y^2/R^2)\mathbf{i}$, where $\mathbf{i}$ is a unit vector along the X-direction, and $\tilde{u}_0$ is the centerline velocity, which may be positive or negative. The channel walls are assumed to be adiabatic. Curved flames are addressed which correspond to traveling-waves in the (X, Y) plane separating the frozen com-

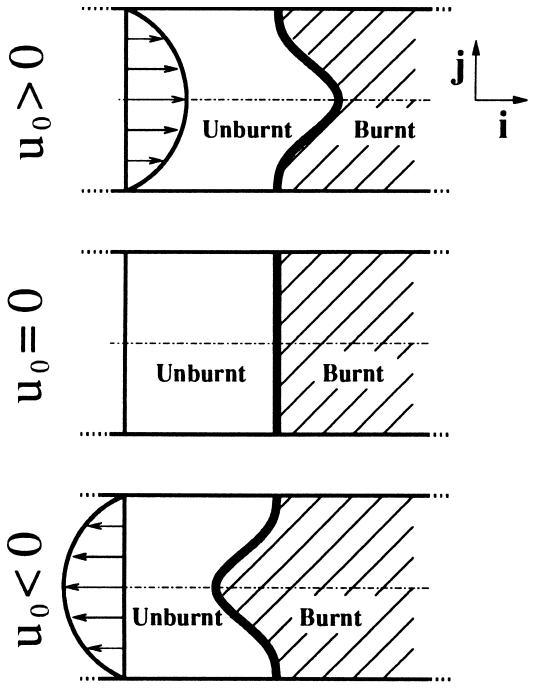

Fig. 2. Flame propagation in a channel under a prescribed Poiseuille flow, with the centerline velocity denoted by u_0. The flame front separates a frozen combustible mixture to the left from combustion products to the right. The subfigures correspond, from top to bottom, to $u_0 > 0$, $u_0 = 0$ and $u_0 < 0$, respectively.

bustible mixture, far to the left, from combustion products to the right. The flames propagate along the X-direction with speed $-\tilde{U}\mathbf{i}$ relative to the channel's wall, a property that remains to be determined. In a frame of reference attached to the flame, the temperature and concentration profiles are time-independent and the velocity field $\mathbf{v}$ is given by $\mathbf{v} = \{\tilde{U} + \tilde{u}_0(1 - Y^2/R^2)\}\mathbf{i}$. A one-step irreversible chemical reaction is adopted which consumes the fuel, considered to be deficient, at a rate given by an Arrhenius law

$$\tilde{\omega} = \rho Y_F B \exp(-E/R^0 T),$$

where B, Y_F, E, R^0, and T represent, respectively, the pre-exponential factor, the mass fraction of fuel, the activation energy, the universal gas constant, and the temperature.

We shall select as unit length the channel half-width R and as unit speed the laminar flame speed $S_L = \sqrt{2\beta^{-2} D_T B \exp(-E/RT_{ad})}$. The expression of S_L is based on the asymptotic approximation for $\beta \gg 1$ of the burning velocity of a planar flame with unity Lewis number Le_F. The Lewis number is defined as the ratio of the thermal diffusivity of the mixture D_T to the fuel diffusion coefficient D_F. Here $T_{ad} = T_u + qY_{Fu}/c_p$ is the adiabatic flame temperature, with the subscript u referring to conditions in the fresh mixture, c_p is the mixture heat capacity and $\beta = E(T_{ad} - T_u)/RT_{ad}^2$ the Zeldovich number. In terms of the normalized mass fraction $y_F = Y_F/Y_{Fu}$ and temperature $\theta = (T - T_u)/(T_{ad} - T_u)$, the dimensionless governing equations are

$$[U + u_0(1 - y^2)] \frac{\partial y_F}{\partial x} = \epsilon Le_F^{-1} \Delta y_F - \epsilon^{-1}\omega \tag{1}$$

$$[U + u_0(1 - y^2)] \frac{\partial \theta}{\partial x} = \epsilon \Delta \theta + \epsilon^{-1}\omega, \tag{2}$$

where ϵ is the ratio of the planar flame thickness $l_{Fl} = D_T/S_L$ to the reference length R, and $U = \tilde{U}/S_L$, $u_0 = \tilde{u}_0/S_L$ are the scaled propagation speed and centerline velocity, respectively. The nondimensional reaction rate ω is given by

$$\omega = \frac{\beta^2}{2} y_F \exp\left\{\frac{\beta(\theta - 1)}{1 + \alpha(\theta - 1)}\right\}, \tag{3}$$

where $\alpha \equiv (T_{ad} - T_u)/T_{ad}$ is the heat-release parameter.

The boundary conditions adopted are

$$y_F = 1, \qquad \theta = 0 \quad \text{as} \quad x \to -\infty, \tag{4}$$

$$\frac{\partial y_F}{\partial x} = \frac{\partial \theta}{\partial x} = 0 \quad \text{as} \quad x \to \infty, \tag{5}$$

corresponding to the frozen conditions in the fresh mixture and the uniform (x-independent) conditions far downstream, and

$$\frac{\partial y_F}{\partial y} = \frac{\partial \theta}{\partial y} = 0 \quad \text{for} \quad y = 0, \tag{6}$$

$$\frac{\partial y_F}{\partial y} = \frac{\partial \theta}{\partial y} = 0 \quad \text{for} \quad y = 1, \tag{7}$$

expressing symmetry and adiabatic conditions at the impermeable walls.

The problem thus formulated can in general be solved numerically; it yields in particular the flame shape and the propagation speed U, which is an eigenvalue, in terms of the param-

eters. A physically significant quantity related to U is the total burning rate (per unit depth)

$$\epsilon^{-1}\int_{-\infty}^{\infty}\int_{-1}^{1}\omega\, dy\, dx \equiv 2\Omega$$

Because of our choice of units, Ω is the total quantity of fuel consumed per unit time in the channel relative to that consumed by a *planar* flame propagating in the same channel. Integrating Eq. 1 across the channel using the conditions that fuel does not penetrate through the walls and that the combustion is completed behind the flame, one finds that

$$\Omega = U + \frac{2u_0}{3} \tag{8}$$

Thus, a simple relation exists between the total burning rate Ω, the propagation speed U and flow intensity u_0. For simplicity, we shall be mainly concerned here with unity Lewis number and concentrate on the influence of the parameters ϵ and u_0. Two related parameters, are the Peclet number

$$Pe \equiv \frac{|\tilde{u}_0|R}{D_T} = \frac{|u_0|}{\epsilon} \tag{9}$$

representing the ratio of convective-to-conductive heat transfer, and the Damkholer number

$$Da \equiv \frac{R|\tilde{u}_0|^{-1}}{l_F S_L^{-1}} = \frac{1}{\epsilon|u_0|} \tag{10}$$

representing the ratio of diffusion-to-chemical reaction times.

ASYMPTOTIC RESULTS—WEAKLY STRETCHED FLAME

Since the flames under investigation are curved and subject to a nonuniform flow field, their local normal propagation speed is expected to deviate from the laminar flame speed. This deviation is proportional to the Karlovitz stretch

$$\kappa = -\mathbf{n}\cdot\nabla\times(\mathbf{v}\times\mathbf{n}) + (\mathbf{v_f}\cdot\mathbf{n})\cdot(\nabla\cdot\mathbf{n})$$

when κ is small [8, 9]. Here $\mathbf{v}$ and of $\mathbf{v_f}$ are the velocity of the fluid and of the flame, respectively, and $\mathbf{n}$ is a unit vector normal to the thin reaction sheet pointing to the burned gas. (In the frame attached to the flame front, considered here, $\mathbf{v_f} = \mathbf{0}$). If the reaction sheet is described by $x = f(y)$, the unit normal is given by $\mathbf{n} = (\mathbf{i} - f'(y)\mathbf{j})/(1 + f'^2)^{1/2}$ and

$$\kappa = \frac{\epsilon}{\sqrt{1+f'^2}}\left[\frac{uf'}{\sqrt{1+f'^2}}\right]' \tag{11}$$

where prime indicates differentiation with respect to y. Note that an ϵ appears in the expression of κ to account for the fact that the length scale used in this study is the channel width rather than the thickness of the planar flame.

For a parallel flow $\mathbf{v} = u(y)\mathbf{i}$ and, in the absence of thermal expansion, one obtains for the flame speed $S_f \equiv \mathbf{v}\cdot\mathbf{n}$ the expression

$$S_f = \frac{u(y)}{(1+f'^2)^{1/2}} = 1 - \left(1 + \frac{le_F}{2}\right)\kappa, \tag{12}$$

where $le_F = \beta(Le_F - 1)$ is a reduced Lewis number. Because the validity of Eq. 12 requires κ to be small, the factor $u(y)/(1 + f'^2)^{1/2}$ is equal to unity in first approximation. Thus $\kappa \approx \epsilon f''/(1 + f'^2)^{1/2}$ and this expression may be used to simplify Eq. 12. In our particular case, $u(y) = U + u_0(1 - y^2)$ leads to the following equation for the slope of the flame front $\Phi \equiv f'(y)$:

$$U + u_0(1 - y^2) = (1 + \Phi^2)^{1/2} - \epsilon\Phi' \tag{13}$$

For simplicity of notation, we have taken $le_F = 0$, but the equation is equally valid for $le_F \neq 0$ if the factor $(1 + le_F/2)$ is absorbed into ϵ. The boundary conditions to be satisfied by Φ are

$$\Phi(0) = 0, \qquad \Phi(1) = 0, \tag{14}$$

expressing a zero slope at the wall and at the centerline (symmetry). Because two boundary conditions are available for the first order differential Eq. 13, the determination of the eigenvalue U along with the flame shape is possible, in principle, in terms of the parameters u_0 and ϵ. The integration may be carried out numerically, for example, by using a shooting method, as reported below. It is instructive, however, to first consider special distinguished limits.

It is worth pointing out that, by integrating the energy Eq. 2 up to the flame front using the

adiabatic condition Eq. 7 and the assumption of complete fuel consumption, one finds

$$\Omega = \int_0^1 \sqrt{1 + \Phi^2}\, dy \tag{15}$$

This implies that the total burning rate is proportional to the flame surface area, a relation first observed by Damköhler [10] in connection with the turbulent flame speed.

Weak flow $u_0 \to 0$ with $\epsilon = O(1)$

Here the leading order solution corresponding to $u_0 = 0$ is obviously the planar flame, $\Phi = 0$ and the propagation speed $U = 1$ (Fig. 2b). A straightforward expansion in powers of u_0 yields

$$\Phi = -\frac{u_0}{3\epsilon}(y - y^3) - \frac{u_0^2}{18\epsilon^3} \cdot \left(\frac{8y}{105} - \frac{y^3}{3} + \frac{2y^5}{5} - \frac{y^7}{7}\right) + o(u_0^2) \tag{16}$$

$$U = 1 - \frac{2u_0}{3} + \frac{4u_0^2}{945\epsilon^2} + o(u_0^2), \tag{17}$$

valid independently of the sign of u_0. Thus, the burning rate

$$\Omega \sim 1 + \frac{4u_0^2}{945\epsilon^2} = 1 + \frac{4}{945} Pe^2 \tag{18}$$

depends only on a single parameter, the Peclet number, and is minimum (equal to unity) when $u_0 = 0$.

Thin flame $\epsilon \to 0$ with $u_0 = O(1)$

Here the sign of u_0 is important, since the derivation depends on the location of the leading edge, which is dictated by this sign. We shall begin with the case $u_0 < 0$, for which the leading edge is at the centerline, $y = 0$ (Fig. 2a). Letting $U = U_0 + \epsilon U_1 + \ldots$, $\Phi = \Phi_0 + \epsilon\Phi_1 + \ldots$ and substituting into Eqs. 13 and 14, we find to leading order in ϵ the equation

$$U_0 + u_0(1 - y^2) = \sqrt{1 + \Phi_0^2} \tag{19}$$

that satisfies the boundary condition at the centerline $\Phi_0(0) = 0$, provided $U_0 + u_0 = 1$. Thus,

$$\Phi_0 = +\sqrt{(1 - u_0 y^2)^2 - 1} \tag{20}$$

where the + sign in front of the square root has been selected so that the flame trails behind its leading edge. To next order we obtain

$$U_1 = \Phi_0\Phi_1/\sqrt{1 + \Phi_0^2} - \Phi_0', \tag{21}$$

which yields, when applied at $y = 0$, the correction to the propagation speed $U_1 = -\Phi_0'(0) = \sqrt{-2u_0}$, and when applied elsewhere, an expression for Φ_1. For the propagation speed and burning rate we may thus write

$$U \sim 1 - u_0 - \sqrt{-2u_0}\,\epsilon \tag{22}$$

$$\Omega \sim 1 - \frac{1}{3}u_0 - \sqrt{-2u_0}\,\epsilon \tag{23}$$

The significance of Eq. 22 is clear: the flame speed at the leading edge, $U + u_0$, is equal to the laminar flame speed plus a correction due to stretch, proportional to ϵ times the square root of the flow intensity u_0.

We note that the boundary condition at the wall, $\Phi(1) = 0$, has not been used; in fact this condition is not satisfied by the approximate solution Eq. 20 except when $u_0 = 0$. To ensure that $\Phi(1) = 0$ the solution must be matched to that in a boundary layer near the wall where Eq. 13 must be reconsidered. The approximate solution Eq. 20, however, provides a satisfactory description of the flame elsewhere. This is particularly true near the leading edge where the local flame shape dictates the value of U as we have seen. More generally, by application of (13) and (14) at $y = 0$ and $y = 1$, one finds $U + u_0 = 1 - \epsilon\Phi'(0)$ and $U = 1 - \epsilon\Phi'(1)$, respectively. It follows that

$$\epsilon\Phi'(1) = \epsilon\Phi'(0) + u_0, \tag{24}$$

which relates the flame curvature, measured in units of the flame thickness l_{Fl}, at the wall and at the centerline. According to Eq. 24, these two curvature cannot be simultaneously small unless u_0 is. In particular, a leading order solution obtained by dropping the contribution of the term $\epsilon\Phi'$ in Eq. 13, cannot be uniformly valid when u_0 is $O(1)$ as in the case under consideration. A uniformly valid description can be

found by matching the solution thus found to an inner solution near the wall where $\epsilon\Phi' = O(1)$. This correction is of little interest since anyway Eq. 13 is physically meaningful only for small values of the flame stretch, i.e., for $\epsilon\Phi' \ll 1$. A similar problem, in a slightly different context, was also noticed in [11].

We turn now to the case $u_0 > 0$, for which the leading edge is located at the wall (Fig. 2c). To leading order Eq. 19 holds and, on using the condition $\Phi_0(1) = 0$, we find $U_0 = 1$ and

$$\Phi_0 = -\sqrt{[1 + u_0(1 - y^2)]^2 - 1}, \tag{25}$$

where the minus sign is chosen so that the flame trails behind its leading edge. To next order we recover Eq. 21, which we apply at $y = 1$ to determine the correction to the propagation speed U_1. One finds that $U_1 \to \infty$, because Eq. 25 implies that

$$\Phi_0 \sim -2u_0^{1/2}\sqrt{1 - y} \quad \text{as} \quad y \to 1^- \tag{26}$$

The straightforward expansion is thus not valid near the wall. The appropriate scaling there is found to be $1 - y = 2\epsilon^{2/3}\eta$ with

$$\Phi = \epsilon^{1/3}\Psi(\eta), \qquad U = 1 + \epsilon^{2/3}U_1,$$

leading to the inner problem

$$\Psi_\eta + \Psi^2 = 8u_0\eta + 2U_1 \tag{27}$$

This equation, supplemented with the boundary condition $\Psi(0) = 0$, and the matching requirement Eq. 26, determine both Ψ and the eigenvalue U_1. Equation 27 is a Ricatti equation, which reduces to the linear Airy equation $P_{\tilde\eta} - \tilde\eta P = 0$ when the substitution $\Psi = P'/P$ and $\tilde\eta = (4u_0\eta + U_1)/2u_0^{2/3}$ is made. The general solution may thus be written in terms of the Airy functions Ai and Bi and their derivatives (denoted by primes) as

$$\Psi = 2u_0^{1/3}\frac{\mathrm{Ai}'(\tilde\eta) + C\mathrm{Bi}'(\tilde\eta)}{\mathrm{Ai}(\tilde\eta) + C\mathrm{Bi}(\tilde\eta)}, \tag{28}$$

where C is an arbitrary constant. This expression satisfies the matching condition Eq. 26 only if $C = 0$ because only then

$$\Psi = 2u_0^{1/3}\frac{\mathrm{Ai}'(\tilde\eta)}{\mathrm{Ai}(\tilde\eta)} \tag{29}$$

has the correct asymptotic behaviour $\Psi \sim -2u_0^{1/2}\sqrt{2\eta}$ as $\eta \to \infty$. By using Eq. 29, we apply now the boundary condition $\Psi(0) = 0$ which implies that $\tilde\eta^* = U_1/2u_0^{2/3}$ is a zero of the function $\mathrm{Ai}'(\tilde\eta)$. Among the infinitely many zeros of Ai′ we select the largest value ≈ -1.02 because otherwise Ψ would change sign at multiple locations and the flame will have multiple tips (where $\Psi = 0$) in the inner layer. Therefore, the propagation speed is given by

$$U \sim 1 - 2Au_0^{2/3}\epsilon^{2/3} \tag{30}$$

$$\Omega \sim 1 + \frac{2}{3}u_0 - 2Au_0^{2/3}\epsilon^{2/3} \tag{31}$$

with $A \approx 1.02$. Again the flame speed at the leading edge U is equal to the laminar flame speed plus a small stretch-correction, but now proportional to the product $u_0\epsilon$ raised to the power 2/3, or $Da^{-2/3}$. Finally, we note that the boundary condition at the centerline, $\Phi(0) = 0$, is not satisfied by the solution Eq. 25 as is to be expected from the remarks given above.

At this stage, it is appropriate to check the results against numerical solutions of Eqs. 13 and 14 obtained by a shooting method. The comparison is presented in Fig. 3 where the burning rate Ω, given by Eqs. 8 or 15, is plotted against u_0 for selected values of ϵ. The solid straight lines in this figure are the leading terms in the asymptotic expressions 22 and 30, for small ϵ. For given u_0 the burning rate decreases when increasing ϵ and the corrections terms, proportional to $|u_0|^{1/2}$ for $u_0 < 0$ and to $u_0^{2/3}$ for $u_0 > 0$, are in agreement with the trend depicted by the numerical results. The solid parabolas correspond to the leading order solution 18 for small u_0, with ϵ equal to 0.5 (upper parabola) and 1 (lower one). It is seen that the asymptotic expressions are indeed consistent with the numerical results. In particular, for a fixed ϵ the profile of Ω vs. u_0 is parabolic for small u_0, which implies that the increase in burning rate as a result of a sufficiently weak flow is the same whether the flow is directed towards or against the direction of propagation. For stronger flow intensities, the burning rate Ω increases linearly with u_0 in both cases but the rate of increase is higher if $u_0 > 0$. These conclusions will be confirmed by the numerical analysis of the full problem presented next.

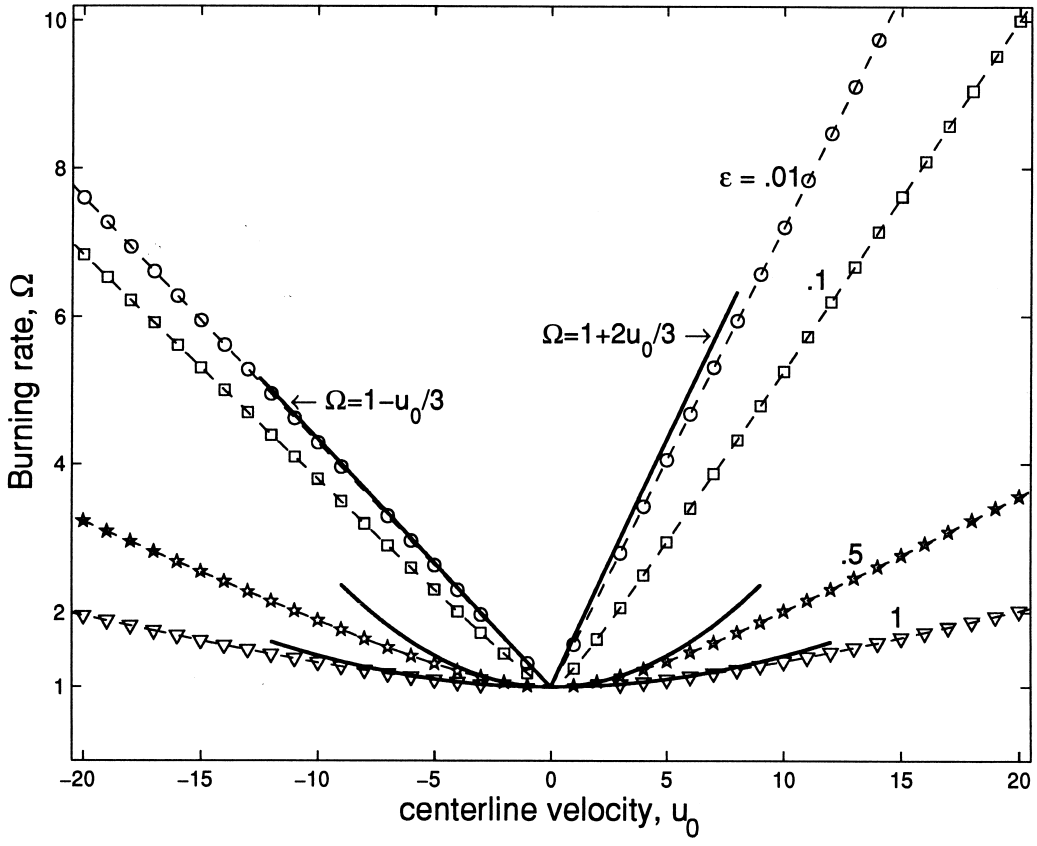

Fig. 3. Burning rate Ω vs. u_0 for selected values of ϵ obtained from the numerical solution of the ODE 13. The solid straight lines are the leading terms in the asymptotic expressions for small ϵ; the solid-curve parabolas correspond to the asymptotic expression for small u_0 with ϵ equal to 0.5 (upper parabola) and 1 (lower one).

NUMERICAL RESULTS—SIGNIFICANTLY STRETCHED FLAME

In this section, we present numerical solutions of the two-dimensional problem consisting of Eqs. 1 and 2 subject to boundary conditions 4 through 7. The numerical method is based on a finite-volume discretization of the governing equations in their steady-state form, which leads to a linear system of equations at every step of the iteration. The propagation speed is updated iteratively so that the flame remains fixed in the computational domain. The (non-dimensional) size of the latter is 1 in the y-direction and 500ϵ in the x-direction. The grid is rectangular but non-uniform with typically 800×100 points.

In the calculations presented below we examine the influence of varying ϵ and u_0 with the other parameters assigned the fixed values $Le = 1$, $\beta = 8$, and $\alpha = 0.85$.

We begin by an illustrative case, depicted in Fig. 4, corresponding to a fixed value of $\epsilon = 0.1$ subject to different flow intensities u_0. This case corresponds to a relatively thin flame, or a wide tube. In the figure, the value of u_0 increases from negative to positive, as we move from top to bottom. The flame is characterized by two iso-temperature contours, namely $\theta = 0.4$ and $\theta = 0.8$; the adiabatic flame temperature corresponds to $\theta = 1$. In all cases, the burned gas lies to the right of the flame. The direction of propagation is to the left, except when it is explicitly indicated that $U < 0$; then the flame moves to the right. When $u_0 = 0$ the flame is planar and propagates to the left into the quiescent unburned gas at the laminar flame speed ($U = 1$). In the presence of a weak flow, the flame still propagates as a whole to the left, but is now curved; its central part is pointing towards the burned gas when $u_0 > 0$ so that the

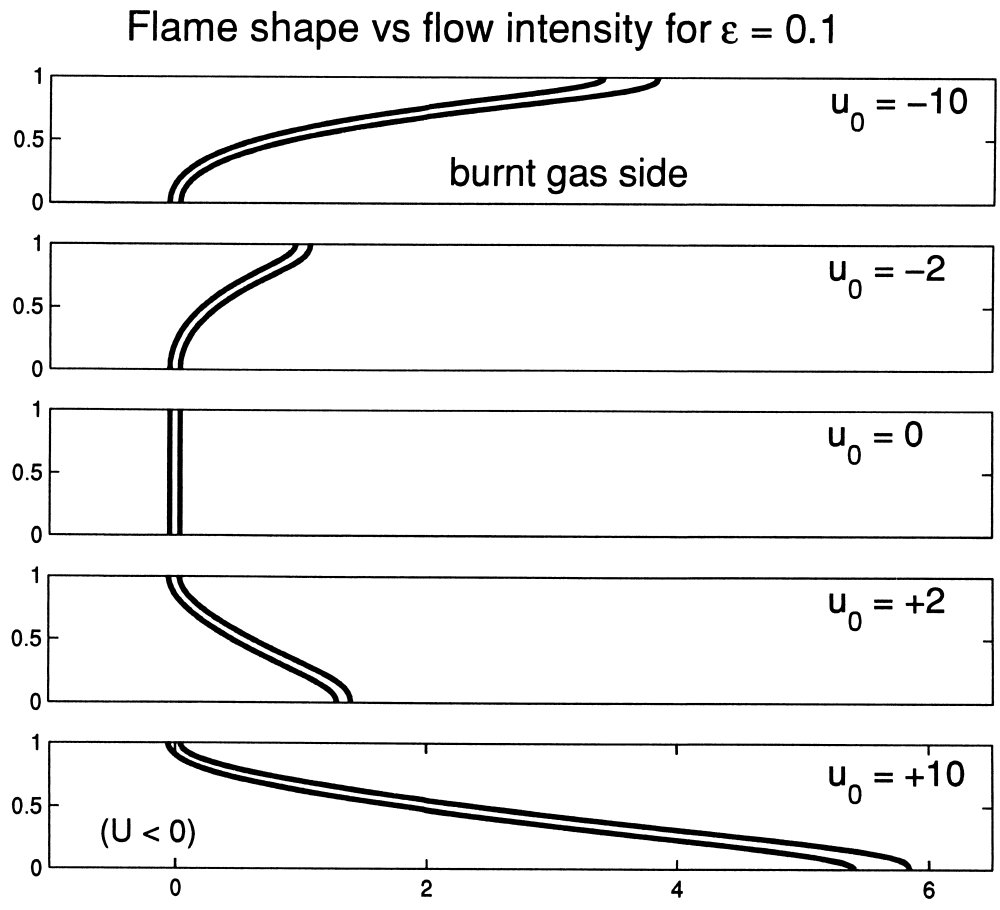

Fig. 4. Flame shape for $\epsilon = 0.1$ and selected values of u_0. Each flame is represented by two iso-temperature contours, $\theta = 0.4$ and $\theta = 0.8$. The flames propagate to the left, relative to the channel wall ($U > 0$), except when explicitly indicated.

leading edge is at the wall, and towards the unburned gas when $u_0 < 0$ so that the leading edge is at the center of the tube. The burning rate, proportional to the flame surface area (see Eq. 15) is nearly equal in both cases and is independent of the sign of u_0, which is well captured by the leading term of the expansion 18. By increasing the magnitude of the flow the flame continues to propagate to the left, when $u_0 < 0$, with an increasing velocity U; it is being blown off by the flow. When $u_0 > 0$, however, the direction of propagation eventually changes and for large enough u_0 the flame propagates to the right (see for example the last subfigure in Fig. 4). A negative value of U implies that the leading edge of the flame, which is located in this case at the wall, is retreating relative to the stagnant gas there; i.e., the flame speed at the leading edge is also negative. The critical value, u_0^{cr} say, corresponding to $U = 0$ is the condition necessary to stabilize the flame so that, in order to avoid flashback ($U > 0$), it is required that $u_0 > u_0^{cr}$. Such information is clearly relevant to applications such as Bunsen burners for which, of course, some modifications to our present model are needed. Finally, it is seen, by comparing the first and last subfigures in Fig. 4, that the flame develops more surface area when it is opposed by the flow and thus propagate faster than when it is aided by the flow ($u_0 < 0$). This is clearly consistent with the asymptotic results of Fig. 3, as pointed out earlier.

Figure 5 is similar to Fig. 4 except that now $\epsilon = 1$, corresponding to a narrower tube, or a thicker flame. This is clearly seen in the figure as the distance between the same isotherms, $\theta =$

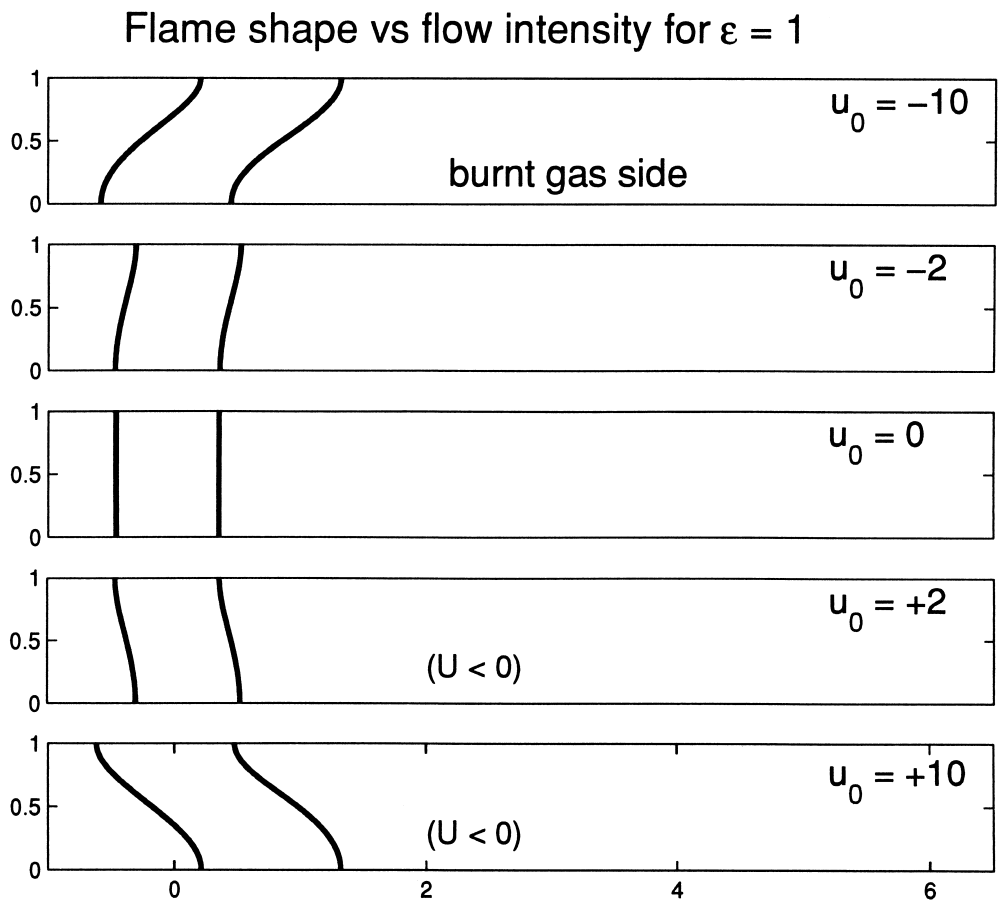

Fig. 5. Same as Fig. 4 but with $\epsilon = 1$.

0.4 and $\theta = 0.8$, are now further apart. We also note that, in this case, the flame deformation from the planar shape is less pronounced. This is to be expected because an increase in ϵ is associated with a decrease in Peclet number (see Eq. 9) which implies that convective transport responsible for flame deformation is strongly opposed by heat conduction that tends to eliminate temperature differences. We also observe that the critical value u_0^{cr}, below which flashback occurs, is now reduced. Negative values of U are more easily attained, as u_0 is increased, when ϵ is large as may be expected from the expression 10 of the Damköhler number.

A summary of the numerical calculations is given in Fig. 6. Shown in this figure is the burning rate Ω vs. u_0 plotted for selected values of ϵ, similar to Fig. 3, which was based on the asymptotic results. For the sake of comparison, we have included the two solid straight lines, corresponding to the leading terms in the asymptotic expansions 22 and 30 for small ϵ, and a solid-line parabola corresponding to the expansion 17 for small u_0, with $\epsilon = 0.5$. The agreement between the numerical and asymptotic results is seen to be very good. In particular, as ϵ goes to zero the numerical curves approach the straight lines, and for fixed $\epsilon = 0.5$, the numerical profiles coincide with the solid-line parabola for small u_0. Again, the numerical results confirm that the rate of increase of Ω with flow intensity is higher if u_0 is positive. Moreover, the profiles switch from being parabolic for small u_0, to become linear for larger (positive or negative) values of u_0. It is quite notable that the simple model considered in the previous section captures all the qualitative features of the problem, even those corresponding to highly stretched flame. The

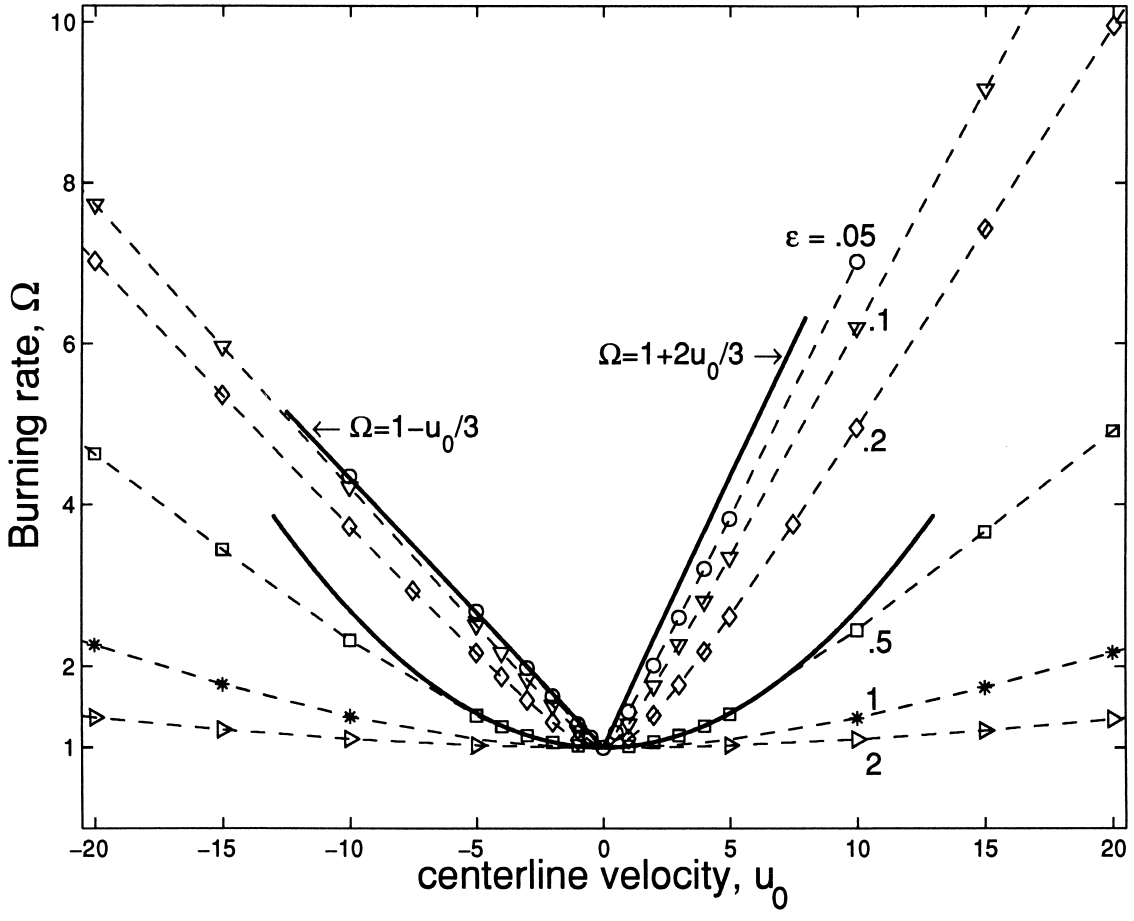

Fig. 6. Burning rate Ω vs. u_0 for selected values of ϵ obtained from the numerical solution of the two-dimensional problem. The solid straight lines are based on the leading terms in the asymptotic expressions for small ϵ; the solid-curve parabola correspond to the asymptotic expression for small u_0 with $\epsilon = 0.5$.

behavior found here presents some similarities with experimental results on turbulent premixed flames [12] where the turbulent flame speed is found to depend quadratically on the intensity of turbulence (the r.m.s. of the fluctuating velocity) if the latter is small, and linearly for larger turbulence levels. The analogy, however, is limited because of the multi-scale nature of turbulence.

The increase in burning rate with u_0 is accompanied by negative flame speeds. This is particularly clear in Fig. 7, where, based on the numerical calculations the flame speed at the leading edge of the flame, denoted by S^*, is plotted against u_0; the flame speed is defined, as usual, as the velocity of the flame relative to the gas velocity of the fresh reactive mixture just ahead of it. Thus, at the leading edge, the flame speed is equal to U for $u_0 > 0$ and $U + u_0$ for $u_0 < 0$ (see Fig. 2). We see in the figure that $S^* = 1$ for $u_0 = 0$ corresponding to a planar flame; it decreases with increasing $|u_0|$, becoming negative as the magnitude of u_0 grows to sufficiently large values. The decrease in flame speed is steeper when the flame thickness, or ϵ, is larger but cannot exceed a critical value. More precisely, the admissible region in the diagram lies below the horizontal line $S^* = 1$, corresponding to an infinitely thin flame ($\epsilon \to 0$), and above the straight solid-lines, corresponding to a thick flame ($\epsilon \gg 1$). The existence of the lower bound is explained by the fact that, for fixed u_0, the burning occurs in a thick but nearly vertical zone as $\epsilon \to \infty$ (see also Fig.

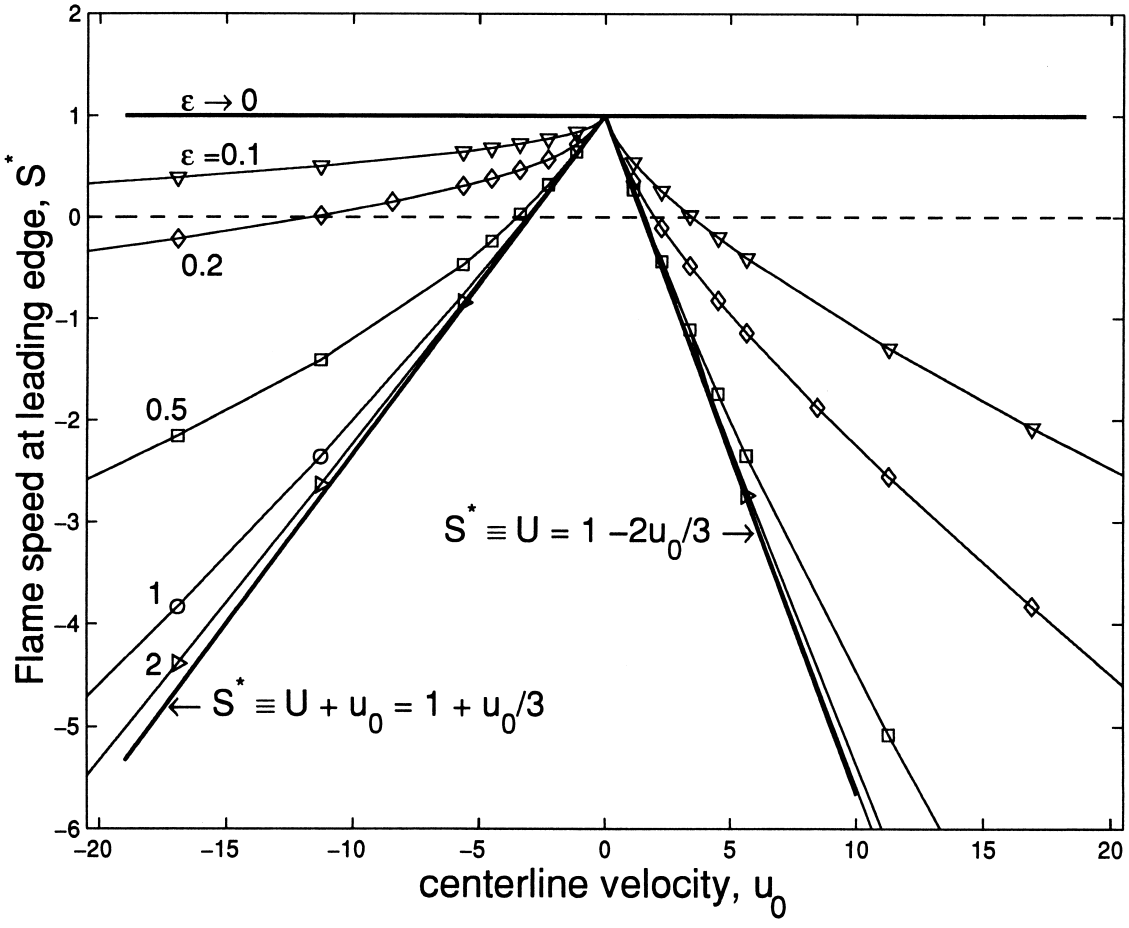

Fig. 7. Flame speed at the leading edge, S^* vs. u_0 for selected values of ϵ.

5). As noted earlier this limit corresponds to $Pe \to 0$ so that $\Omega = U + 2u_0/3 \to 1$.

Concentrating now on the right half of the diagram ($u_0 > 0$) in Fig. 7, the following conclusions can be drawn concerning flame flashback (corresponding to $U > 0$). First, we note that flashback will always occur in an adiabatic channel if $u_0 < 3/2$, or equivalently if the average flow velocity is less than unity. Second, for a given value of ϵ, the diagram determines the critical value u_0^{cr}. The condition $u_0 > u_0^{cr}$ may actually be considered as a sufficient requirement to avoid flashback in all channels whether adiabatic or not, since heat losses would typically lessen the tendency for flashback. Finally, for fixed u_0 a critical ϵ above that flashback will be suppressed can be similarly determined.

We conclude this section by addressing the question raised in the introduction regarding the long-term evolution of an ignition kernel in the flow under consideration (see Fig. 1). More precisely, we would like to determine the speed with which the kernel will grow after an initial transient, namely the velocity of the flame front propagating to the right and aided by the flow relative to that propagating to the left and opposed by the flow. Simple kinematic arguments suggest that this extension speed is given by $(U_1 + U_2)\mathbf{i}$ where U_1 and U_2 are the propagation velocities corresponding to u_0 and $-u_0$, respectively. In Fig. 8 we have plotted this quantity against the Peclet number $Pe = u_0/\epsilon$ for selected values of ϵ. Note that the use of the Peclet number, instead of u_0, makes the different curves collapse to a single curve when Pe is small; $Pe < 5$ say. This result is associated with the parabolic dependence of Ω on u_0/ϵ depicted in Eq. 17, which has also been used to plot the

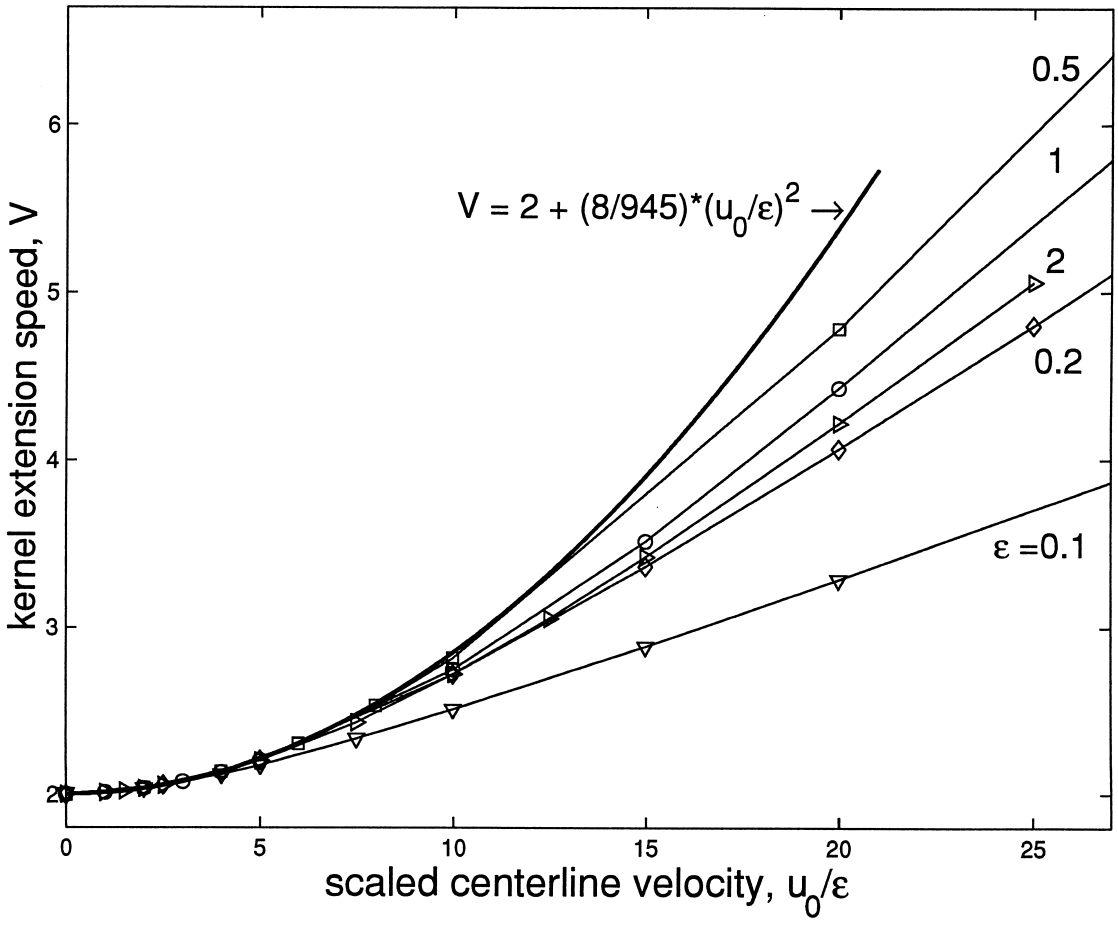

Fig. 8. Extension speed of an ignition kernel, beyond an initial transient state, versus the Peclet number *Pe* for selected values of ϵ.

solid-curve parabola. As u_0 is increased the dependence of the extension speed on *Pe* becomes linear but the slope varies significantly with ϵ. In all cases, the extension speed is larger than two, namely twice the laminar flame speed.

CONCLUSION

We have studied flame propagation in an adiabatic channel under a prescribed Poiseuille flow. The problem has provided a simple framework for the investigation of the combined influence of the intensity of the flow field and its spatial scale on the combustion process. In particular, the dependence of the global combustion rate has been determined in terms of these two parameters, along with the propagation speeds and flame shapes in different distinguished regimes. The results have been used to discuss the flashback conditions in two-dimensional channels (based on negative propagation speeds arguments) and the long-term evolution an ignition kernel in a Poiseuille flow. Additional aspects such as inclusion of heat losses and non-unity Lewis number effects will be addressed in future publications.

This work has been supported partially by the National Science Foundation under grants CTS0074320 and DMS0072588.

REFERENCES

1. Lewis, B., and Von Elbe, G., *Combustion, Flames and Explosions of Gases*. Academic Press, New York, 1961, ch. V.
2. Zeldovich, Ya. B., Barenblatt, G. I., Librovich, V. B.,

and Makhviladze, G. M., *Mathematical Theory of Combustion and Explosions*. Plenum Press, New York, 1985, p. 442.
3. Kagan, L., and Sivashinsky, G., *Phys. Rev. E*, 53:6021 (1996).
4. Dery, R. J., *Proc. Combustion Inst*. 3:235 (1949).
5. Berestyski, H., and Sivashinsky, G., *SIAM J. Appl. Math*. 51:344 (1991).
6. Brailovsky, I., and Sivashinsky, G., *Phys. Rev. E* 51:1172 (1995).
7. Aldredge, R. C., *Combust. Flame* 90:121 (1992).
8. Matalon, M., and Matkowsky, B. J., *J. Fluid Mechanics* 124:239 (1982).
9. Matalon, M., *Combust. Sci. Technol*. 31:169 (1983).
10. Damköhler, G., *Z. Elektrochem*. 46:601 (1940). English translation NACA Tech. Memo. No. 1112 (1947).
11. Sung, C. J., Law, C. K., and Umemura, A., *Proc. Combust. Inst*. 24:205 (1992).
12. Ballal, D. R., and Lefebvre, A. H., *Proc. R. Soc. London A* 344:217 (1975).

Received 4 February 2000; revised 9 June 2000